Tetrahedral structure or chains for liquid water

Teresa Head-Gordon* and Margaret E. Johnson

University of California at San Francisco/University of California at Berkeley Joint Graduate Group in Bioengineering, Berkeley, CA 94720

Edited by Frank H. Stillinger, Princeton University, Princeton, NJ, and approved April 3, 2006 (received for review December 9, 2005)

It has been suggested, based on x-ray absorption spectroscopy (XAS) experiments on liquid water [Wernet, Ph., *et al.* (2004) *Science* 304, 995–999], that a condensed-phase water molecule's asymmetric electron density results in only two hydrogen bonds per water molecule on average. The larger implication of the XAS interpretation is that the conventional view of liquid water being a tetrahedrally coordinated random network is now replaced by a structural organization that instead strongly favors hydrogen-bonded water chains or large rings embedded in a weakly hydrogen-bonded disordered network. This work reports that the asymmetry of the hydrogen density exhibited in the XAS experiments agrees with reported x-ray scattering structure factors and intensities for $Q > 6.5$ Å^{-1}. However, the assumption that the asymmetry in the hydrogen electron density does not fluctuate and is persistent in all local molecular liquid water environments is inconsistent with longer-ranged tetrahedral network signatures present in experimental x-ray scattering intensity and structure factor data for $Q < 6.5$ Å^{-1}.

polarizability | tetrahedral liquid | x-ray absorption spectroscopy | x-ray scattering | hydrogen-bonding

Liquid water is usually classified as a tetrahedral liquid because its coordination number, defined as the area under the first peak of the oxygen–oxygen radial distribution function, $g_{OO}(r)$, increases slightly upon melting of hexagonal ice. Based on a geometric definition of averaging over all O–O pairs closer than the first minimum in $g_{OO}(r)$, a coordination number above four and below five suggests that liquid water preserves much of its ice-like tetrahedral structuring, even as the four directional hydrogen bonds of the solid are distorted upon melting by thermal fluctuations to permit less ideal and more compact hydrogen-bonding arrangements in the liquid. Nonetheless, the first peak of $g_{OO}(r)$ is by definition a highly averaged quantity over a multitude of local 3D water molecule arrangements and is therefore somewhat insensitive to the details of hydrogen-bonding patterns in this first coordination shell.

In principle, x-ray absorption spectroscopy (XAS) is sensitive to local hydrogen-bonding patterns because it primarily probes instantaneous electronic arrangement of waters in the first coordination shell (1–3). Recent XAS and x-ray Raman scattering experiments on liquid water have been interpreted to show that the first coordination shell around a water molecule in the bulk fluid has two hydrogen-bonding partners on average (1, 2). This result was determined by comparing and contrasting the near-edge fine structure of the XAS spectra for liquid water with the same spectral signatures exhibited by hexagonal ice in the bulk, where tetrahedral hydrogen-bonding is unambiguous, and at a prepared I_h surface, which involves a significant fraction (50% or more) of broken hydrogen bonds (1, 3). Because the pre-edge peak in the XAS spectra of liquid water more closely resembles the XAS pre-edge peak of the ice surface, a feature that is largely absent in the XAS spectra of bulk ice, it was concluded that liquid water contains a large number of broken hydrogen bonds (1). A more recent total electron yield near-edge x-ray absorption fine structure spectrum of liquid water led to an alternative conclusion that the pre-edge intensity can be expected even for local tetrahedral structure involving minimally distorted hydrogen-bonding configurations that are more consistent with bulk ice (3).

The XAS experiment reported in ref. 1 was further analyzed by simulating the XAS spectra using core excited electronic state estimates from density function theory (DFT), overlayed on putative local hydrogen-bonding configurations of small water clusters that varied between full tetrahedral hydrogen-bonding through to broken donor hydrogen bonds (1). Wernet *et al.* (1) conclude that the configurations most consistent with the appearance of a pre-edge peak in the simulated near-edge fine structure absorption spectra for liquid water [assuming their full core hole density function theories are adequate, which is currently a matter of debate (2, 4, 5)] are ones in which there are "broken" hydrogen bonds. Whether these hydrogen bonds would be classified as broken under other geometric or energetic criteria has been questioned (3, 6).

The classification of a broken hydrogen bond used by Wernet *et al.* (1) was derived from the electronic structure calculations, which showed a shift of electron density concentrated in the hydrogen bond formed between an acceptor oxygen and the donor hydrogen (H_1 in Fig. 1) onto the donor's covalently bonded oxygen and sister hydrogen (H_2 in Fig. 1). The additional electron density on hydrogen H_2 diminishes its capability to hydrogen-bond to other water molecules. This effect results in an average local environment in the liquid in which a water participates in one strong donor and one strong acceptor hydrogen bond on average (Fig. 1). Such configurations were compared with the experimentally derived first peak of $g_{OO}(r)$ (7, 8) and other experimentally derived partial radial distribution functions (9), and Wernet *et al.* (1) assert that they agree well with the reported static structural data. Thus, although the coordination number around a given water molecule can be as high as five, it should not involve more than two hydrogen bonds according to this interpretation of the XAS experiment (1).

An additional assumption in the interpretation of the XAS data is that the instantaneous asymmetric electronic configuration in the first coordination shell of liquid water is a long-lived feature that persists irrespective of a given water's local electronic environment (1). This assumption is to be contrasted with the standard view of liquid water in which the asymmetry in water's electron density arises from variations in electronic environments that fluctuate rapidly on the femtosecond timescale (10, 11). When ensemble averaged, the XAS interpretation assumes that the hydrogen electron density is a sharp bimodal distribution, whereas the standard view is that the hydrogen electron density is a broad unimodal and symmetric distribution. The larger implication of a first coordination shell with two hydrogen bonds is that the conventional view of liquid water being a tetrahedrally coordinated random network must now be replaced by a liquid structural organization with hydrogen-bonded chains or large rings of water molecules embedded in a

Conflict of interest statement: No conflicts declared.

This paper was submitted directly (Track II) to the PNAS office.

Abbreviation: XAS, x-ray absorption spectroscopy.

*To whom correspondence should be sent at the present address: Department of Chemistry, Cambridge University, Lensfield Road, Cambridge CB2 1EW, United Kingdom. E-mail: tlhead-gordon@lbl.gov.

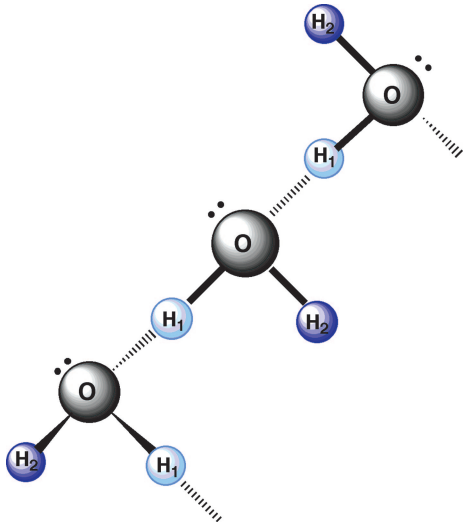

Fig. 1. Cartoon of hydrogen-bonding patterns in the first coordination shell for ambient liquid water as interpreted from XAS data (1, 2). The dashed lines are hydrogen bonds, the solid lines are covalent bonds, and the dots represent oxygen lone pairs. The darker shading for the H_2 hydrogen represents that it is more electronegative than H_1 and hence has reduced hydrogen-bonding capability. The figure was generated with CHEMDRAW ULTRA 10.0 (CambridgeSoft, Cambridge, MA).

weakly hydrogen-bonded disordered network (1), so that tetrahedral order is (effectively) absent.

If this new viewpoint advocated by the XAS experiments is true, it should be consistent with other experimental probes that report on liquid water structure. One of the primary strengths of x-ray (and neutron) scattering is that it generates a static average over both small and large lengthscale correlations in the liquid, whereas the XAS experiment by contrast primarily probes only instantaneous small lengthscale hydrogen-bonding arrangements. This work examines the question of whether a static asymmetric hydrogen charge density model of liquid water actually agrees with x-ray scattering measurements we have reported in refs. 7, 8, 12, and 13, while also agreeing with neutron-scattering data (9, 14) that is most sensitive to OH and HH correlations.

Theoretical and Experimental Background

X-ray scattering is an experimental technique that characterizes the time-averaged structural organization of atoms or molecules in a liquid or solid. X-rays are scattered by the electron density of an atom or molecule, and the scattering cross-section or intensity increases in direct proportion to the number of electrons or atomic number, Z. The expression used for the water scattering intensity in this work is

$$I(Q) = \sum_{ij} x_i x_j f_i(Q) f_j(Q) \frac{\sin Qr_{ij}}{Qr_{ij}} + \sum_{i \leq j} x_i x_j f_i(Q) f_j(Q) H_{ij}(Q), \qquad [1]$$

where $Q = 4\pi \sin(\theta/2)/\lambda$ is the momentum transfer, λ is the radiation wavelength, x_i is the atomic fraction of atom type i, $f_i(Q)$ is the Q-dependent atomic scattering factor for atom type i, and r_{ij} is the intramolecular distance between atom centers i and j. We note our use of an "effective" Bragg spacing d (effective because we are analyzing a liquid and not a crystal) in *Results*, which is given by

$$d = \frac{\lambda}{2 \sin(\theta/2)} = \frac{2\pi}{Q}, \qquad [2]$$

and thus provides a measure of prominent real-space lengthscales in the liquid.

For molecular liquids like water, it is convenient to separate the scattering intensity, $I(Q)$, into two contributions as shown in Eq. **1**. The first term corresponds to scattering contributions from individual molecules due to their intramolecular correlations. The assumption is commonly made that the Z-dependent atomic scattering factors can be represented as scattering from independent neutral atoms, each with a spherical electron density distribution. Our work in ref. 8 derived a more realistic estimate of $f_i(Q)$ values that accounted for chemical bonding in the water molecule, resulting in a net shift of electron density away from the hydrogens onto the oxygen, and reproducing the known molecular form factor (the first term in Eq. **1**) for gas-phase water.

The second term in Eq. **1** is the intensity arising from intermolecular correlations in the liquid. The $H_{ij}(Q)$ values are intermolecular structure factors that are related to real-space intermolecular correlations through the Fourier transform

$$H_{ij}(Q) = 4\pi\rho \int_0^\infty r^2 dr (g_{ij}(r) - 1) \frac{\sin Qr}{Qr}, \qquad [3]$$

where ρ is the atomic density and $g_{ij}(r)$ is the radial distribution function describing spatial density correlations between atom types i and j. Based on the use of modified atomic form factors that were suitably modified for the liquid (8), we have shown that ≈85% of liquid water's scattering intensity is due to oxygen–oxygen correlations, and ≈15% is due to oxygen–hydrogen correlations, whereas hydrogen–hydrogen correlations contribute negligibly to the intensity signal (7, 8, 12). Given the now-correct weighting of the intermolecular intensity contributions, our approach allows for extraction of a $g_{OO}(r)$ (8). Our approach for extracting an experimental $g_{OO}(r)$ and $g_{OH}(r)$ involved finding the optimal linear combination of real space functions, a "basis set" of radial distribution functions culled from water simulations, various experimental curves, and integral equation theories, to best fit the experimental data (8). In summary, the experimental intensity can be manipulated to yield partial structure factors or radial distribution functions, and vice versa, by using Eqs. **1** and **3**.

The asymmetric model of water liquid structure (ref. 14 and A. K. Soper, personal communication) is derived from a computational technique known as the empirical potential structure refinement (EPSR) (15). The EPSR method perturbs a reference potential for liquid water by using the experimental structure factors as constraints that are ultimately satisfied within some refinement error (15, 16). In ref. 14, an asymmetric reference potential was defined in which the charges of the SPC/E model (17) are shifted so that $q_{H_1} = 0.6e$, $q_{H_2} = 0.0e$, and $q_O = -0.6e$, resulting in a 3D model of the liquid in which the mean number of hydrogen bonds is 2.2 per water molecule (Fig. 1). No evidence exists yet that shows that such an asymmetry in charge distribution could result in a model of water that adequately reproduces the global thermodynamic, dynamic, or dielectric properties of the liquid. However, such asymmetry in charge can be used to produce a model of water that approximates the binding energy reasonably well (14) and by construction is as consistent with both the x-ray and neutron structure factors as minimizing the refinement error permits (14).

The structure factor data for the asymmetric model of water reported in ref. 14 does not show good agreement with our x-ray scattering experiment. This lack of agreement is due to errors in

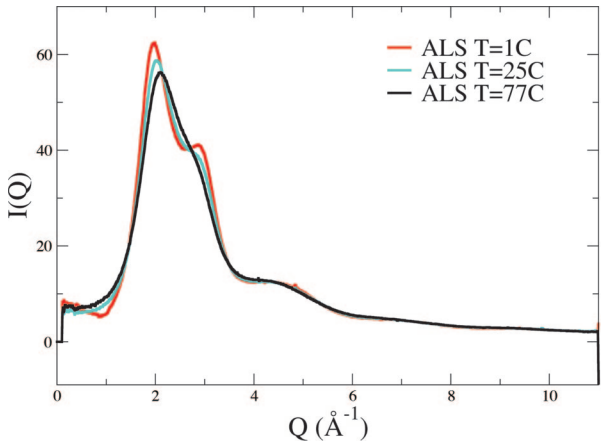

Fig. 2. The experimental x-ray intensity of liquid water as a function of temperature (12). Red line, 1°C; blue line, 25°C; black line, 77°C. The shoulder region near $Q \approx 3.0$ Å^{-1} involves a structural feature in the first coordination shell (effective Bragg spacing of ≈2.0 Å) that tracks tetrahedral structure in the water liquid as a function of temperature.

the handling of the x-ray data with regards to normalization, neglect of proper weightings of partial structure factors using the modified atomic form factors reported in ref. 8, and using structure factor data reported in ref. 7 instead of the more recent intensity data that extends to higher Q that is reported in ref. 12. The conclusions drawn in ref. 14 about the inadequacy of our reported x-ray data for $Q > 6.0$ Å^{-1} is clearly a result of this mishandling of the experimental data reported in refs. 7, 8, and 12, and will be addressed in a future erratum (A. K. Soper, personal communication).

It was concluded in ref. 14 that the asymmetric model agrees adequately with the neutron scattering data, except for differences at low-Q that were thought to be attributable in part to intractable removal of inelastic scattering. Therefore, an important conclusion of ref. 14 is that the neutron data cannot distinguish between a symmetric model versus an asymmetric model of liquid water. By contrast, the x-ray data were thought to exhibit clear differences between the two models that might shed light on the results and conclusions drawn from the XAS study (1).

Results

Fig. 2 shows the intensity profile over the range of 0.4 Å$^{-1} < Q < 10.8$ Å^{-1} for liquid water at different temperatures taken at the Advanced Light Source that we reported in 2003 (12), improved experiments that went out further in momentum transfer than the original experiments reported in 2000 (7, 8). The main intensity peak at $Q = 2.0$ Å^{-1} of room-temperature water is consistent with an effective Bragg spacing between oxygens of ≈3.1 Å and shifts to smaller (larger) Q with decreasing (increasing) temperature (Fig. 1). More local structural order in the first coordination shell is manifest in the intensity profile at higher momentum transfer near $Q \approx 3.0$ Å^{-1} (effective Bragg spacing of ≈2.0 Å), which shows a shoulder feature at room temperature (7, 8, 12). Because this feature sharpens as the temperature of the liquid is lowered to 1°C (a temperature just above that at which hexagonal ice forms) or melts out at higher temperature as shown for water at 77°C, it correlates empirically with gain or loss of tetrahedral structure in the water network (Fig. 2).

Fig. 3*a* shows a comparison of the oxygen–oxygen partial structure factor, $H_{OO}(Q)$, from the Advanced Light Source x-ray scattering experiment reported in 2003 (12) with the asymmetric model derived using the empirical potential structure refinement

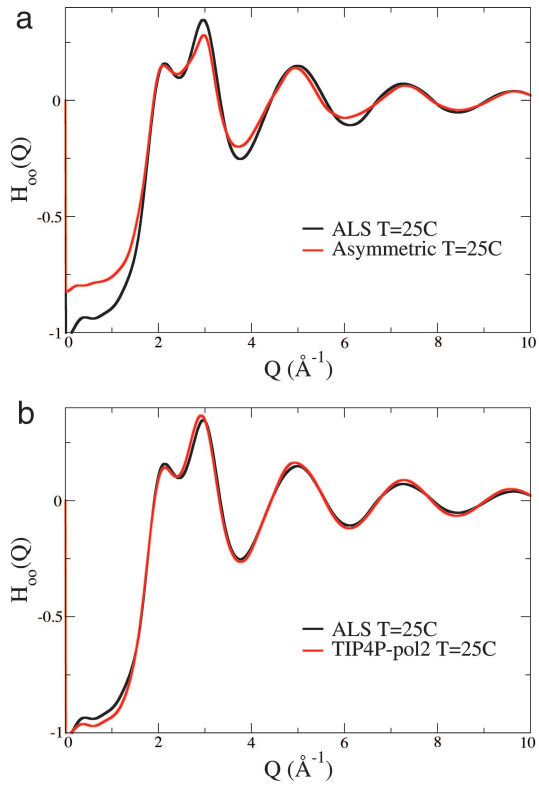

Fig. 3. Comparison of $H_{OO}(Q)$ structure factors from experiments reported in ref. 12 (black) against the asymmetric water model (ref. 14; red) (*a*) and the classical polarizable TIP4P-pol2 model (ref. 16; red) (*b*). The simulated structure factors using the asymmetric and TIP4P-pol2 models show good agreement with x-ray scattering for $Q > 6.5$ Å^{-1}. However, the simulated structure factors for the asymmetric model shows significant disagreement for $Q < 6.5$ Å^{-1}, whereas the TIP4P-pol2 model shows excellent agreement over the full Q range of the measured x-ray data.

method and kindly supplied to us by A. K. Soper (ref. 14 and personal communication). For comparison, in Fig. 3*b* we show $H_{OO}(Q)$ for the polarizable TIP4P-pol2 model (18) that permits hydrogen charge inequalities depending on the local condensed-phase environment but that does not assume that these charge inequalities are static as is the underlying assumption of the asymmetric model (1).

Both models perform exceptionally well against experiment in the high Q region. However, the excellent agreement of both models with experiment for $Q > 6.5$ Å^{-1} means that our x-ray liquid diffraction data are unable to distinguish between a sharp bimodal distribution from a broader unimodal and symmetric distribution of hydrogen electron density. Although higher Q data might distinguish between them, it is unimportant, because it is evident that the asymmetric model disagrees with the x-ray structure factor data for $Q < 6.5$ Å^{-1}, the region of the intensity that contains information about longer-ranged spatial correlations in the liquid. By contrast, the simulated structure factor from the TIP4P-pol2 polarizable model shows excellent agreement with experiment over the full Q-range.

Fig. 4 presents the experimental $g_{OO}(r)$ and the $g_{OO}(r)$ for the asymmetric model to show their differences in terms of real-space correlations. Integrating under the first peak of $g_{OO}(r)$, we find a coordination number of 4.7 from experiment, consistent with preservation of significant tetrahedral structure in the ambient water liquid, whereas the asymmetric model gives a higher coordination number of ≈5.3. The second peak of the experimental $g_{OO}(r)$ describes a smooth distribution of distances centered at ≈4.5 Å, consistent with second neighbor distances in

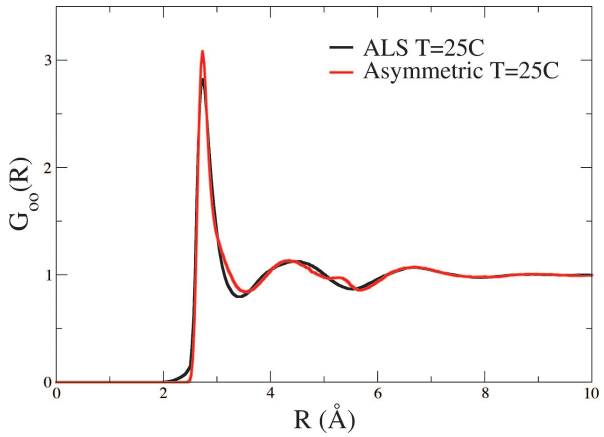

Fig. 4. Comparison of g_{OO}(r) from experiment (12) (black) and the asymmetric model (14) (red) of liquid water at room temperature. The differences in the structure factors of the asymmetric model with experiment shown in Fig. 3*a* are manifest in the $g_{OO}(r)$ as odd substructure in the second peak, with the feature at $r = 5.6$ Å due to a linear arrangements of oxygens as shown in Fig. 1.

which a tetrahedral angle is formed by two oxygens coordinated with the same third oxygen at the vertex. However, the second peak of $g_{OO}(r)$ in the asymmetric model shows unexpected substructure, where presumably the feature at $r = 5.6$ Å in the $g_{OO}(r)$ correlates with a linear arrangement of three oxygens as caricatured in Fig. 1.

We now use the partial radial distribution functions and the Fourier transform defined in Eq. **3** to simulate the intensity, $I(Q)$, as described in Eq. **1**. Fig. 5 shows the resulting simulated intensity for the asymmetric model compared with the direct experimental intensity observable. For the asymmetric model, we have distinct hydrogens so that we can compare simulated intensities using either the $g_{OH1}(r)$ or $g_{OH2}(r)$ as shown in Fig. 5*a*, whereas Fig. 5*b* shows the simulated intensity based on a simple average of the two OH correlations. The OH correlation from the more electronegative hydrogen should have more weight in the x-ray scattering intensity (see *Theoretical and Experimental Background*), and hence the simulated intensity for the asymmetric model should more closely resemble the red curve in Fig. 5*a* relative to Fig. 5*b*. In either case, the differences between the experiment and asymmetric model is seen to be attributable to the asymmetric model's clear diminishment of the characteristic signature for tetrahedral structure in the liquid at $Q \approx 3.0$ Å^{-1} as shown in Fig. 2. The $Q \approx 3.0$ Å^{-1} shoulder of the intensity profile is a feature that is clearly present in the TIP4P-pol2 model as shown in ref. 11 and as is evident by its excellent agreement with the experimental structure factor in Fig. 3*b*. The poor agreement of the asymmetric model with experiment clearly indicates that it is the underlying assumption of a static asymmetry in hydrogen electron density when interpreting the XAS data that is in error.

Discussion

This work demonstrates excellent agreement of simulated structure factors with experimental x-ray structure factors for $Q > 6.5$ Å^{-1} for both a static asymmetric hydrogen electron density model of water and a polarizable model of water. However, our x-ray liquid diffraction experiment may be unable to distinguish between ensemble structural averages that exhibit a sharp bimodal distribution and a broader, unimodal, and symmetric hydrogen electron density distribution. Although even higher Q-data may resolve this difference, it is not needed. We have shown that the assumption of static asymmetry in hydrogen

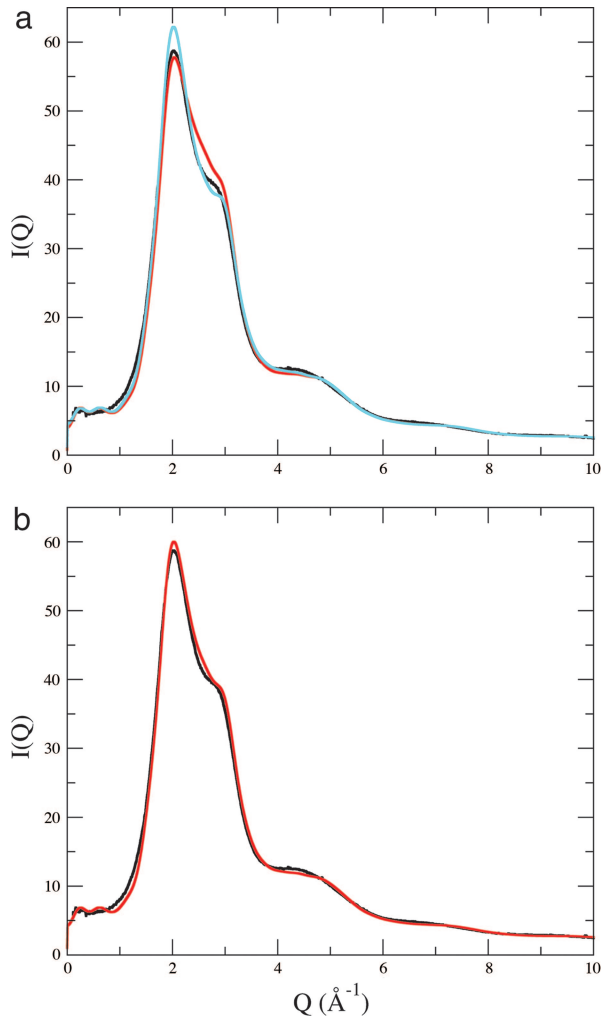

Fig. 5. The comparison of x-ray intensities from experiment (12) (black) and simulated using the asymmetric model (14). (*a*) Using only $g_{OH_1}(r)$ (blue) or only $g_{OH_2}(r)$ (red). (*b*) Using the average of g_{OH_1}(r) and $g_{OH_2}(r)$ (red). Differences with experimental intensities are evident in the main diffraction peak and a loss of the shoulder feature at $Q \approx 3.0$ Å^{-1}, which correlates with a breakdown of tetrahedral structure in the liquid.

electron density is inconsistent with the tetrahedral network signatures present in the experimental x-ray scattering data for $Q < 6.5$ Å^{-1} (outside the window of observation of the XAS experiment).

The deduction from the XAS experiments and interpretation that asymmetry is a time-invariant feature of the hydrogen electron density means that liquid water should organize into strongly hydrogen-bonded water chains or large rings embedded in a weakly hydrogen-bonded disordered network (1). In fact, ring statistics generated in ref. 14 based on the asymmetric model showed that 15-member hydrogen-bonded rings were as probable as the 5- and 6-membered rings that usually dominate in a tetrahedral view of liquid water. Polarizable water models based on fluctuating charges also exhibit asymmetry in charge distributions but only transiently in response to a given local hydrogen-bonding arrangement (9, 10). However, the TIP4P-pol2 polarizable model's excellent agreement with x-ray scattering structure factors over all Q indicates that no specific asymmetry persists and thus is consistent with tetrahedral structure signatures in intensities (12) and analysis of ring statistics.

Our best understanding of liquid water at present is that charge asymmetry in water's electron density arises from symmetry-breaking environments that fluctuate rapidly on the femtosecond timescale (10, 11). Although these instantaneous asymmetries may be seen in an XAS experiment (11), the long timescale (or ensemble) averages inherent in bulk structural experiments such as x-ray scattering tell us that they do not persist, as we have shown here. It is thus important to reconcile the XAS data with a symmetric charge density approximation to the fluctuating charge environments that still remains most compatible with our view of water as a tetrahedral hydrogen-bonded liquid.

We thank Dr. Alan Soper for supplying radial distribution functions and structure factors for the asymmetric model and Drs. Ruth Lynden-Bell and Martin Head-Gordon for interesting discussions and careful reading of the manuscript. T.H.-G. was supported by a Schlumberger Fellowship while on sabbatical at the University of Cambridge and also by the Department of Energy/Basic Energy Sciences Condensed Phase and Interfacial Molecular Sciences program.

1. Wernet, Ph., Nordlund, D., Bergmann, U., Cavalleri, M., Odelius, M., Ogasawara, H., Naslund, L. A., Hirsch, T. K., Ojamae, L., Glatzel, P., *et al.* (2004) *Science* **304,** 995–999.
2. Cavalleri, M., Odelius, M., Nordlund, D., Nilsson, A. & Pettersson, L. G. M. (2005) *Phys. Chem. Chem. Phys.* **7,** 2854–2858.
3. Smith, J. D., Cappa, C. D., Wilson, K. R., Messer, B. M., Cohen, R. C. & Saykally, R. J. (2004) *Science* **306,** 851–853.
4. Hetényi, B., De Angelis, F., Giannozzi, P. & Car, R. (2004) *J. Chem. Phys.* **120,** 8632–8637.
5. Prendergast, D., Grossman, J. C. & Galli, G. (2005) *J. Chem. Phys.* **123,** 14501–14511.
6. Mantz, Y. A., Chen, B. & Martyna, G. J. (2005) *Chem. Phys. Lett.* **405,** 294–299.
7. Hura G., Sorensen, J. M., Glaeser, R. M. & Head-Gordon, T. (2000) *J. Chem. Phys.* **113,** 9140–9148.
8. Sorensen, J. M., Hura, G., Glaeser, R. M. & Head-Gordon, T. (2000) *J. Chem. Phys.* **113,** 9149–9161.
9. Soper, A. K. (2000) *Chem. Phys.* **258,** 121–137.
10. Eaves, J. D., Loparo, J. J., Fecko, C. J., Roberts, S. T., Tokmakoff, A. & Geissler, P. L. (2005) *Proc. Natl. Acad. Sci. USA* **102,** 13019–13022.
11. Fernandez-Serra, M. V. & Artacho, E. (2006) *Phys. Rev. Lett.* **96,** 016404.
12. Hura, G., Russo, D., Glaeser, R. M., Krack, M., Parrinello, M. & Head-Gordon, T. (2003) *Phys. Chem. Chem. Phys.* **5,** 1981–1991.
13. Head-Gordon, T. & Hura, G. (2002) *Chem. Rev.* **102,** 2651–2670.
14. Soper, A. K. (2005) *J. Phys. Condens. Matter* **17,** 1–10.
15. Soper, A. K. (1996) *Chem. Phys.* **202,** 295–306.
16. Soper, A. K. (2001) *Mol. Phys.* **99,** 1503–1516.
17. Berendsen, H. J. C., Grigera, J. P. & Straatsma, T. P. (1987) *J. Phys. Chem.* **91,** 6269–6271.
18. Chen, B., Xing, J. H. & Siepmann, J. I. (2000) *J. Phys. Chem. B* **104,** 2415–2423.